

Growth and Properties of Single Crystals of Noncentrosymmetric $\text{Na}_3\text{VO}_2\text{B}_6\text{O}_{11}$

Xiaoyun Fan,^{†,‡} Shilie Pan,^{*,†} Xueling Hou,[†] Xuelin Tian,[†] and Jian Han[†]

[†]Xinjiang Key Laboratory of Electronic Information Materials and Devices, Xinjiang Technical Institute of Physics & Chemistry, Chinese Academy of Sciences, Urumqi 830011, China, and [‡]Graduate University of Chinese Academy of Sciences, Beijing 100049, China

Jacob Haag and Kenneth R Poepelmeier

Department of Chemistry, Northwestern University, 2145 Sheridan Road, Evanston, Illinois 60208

Received July 28, 2009; Revised Manuscript Received October 20, 2009

ABSTRACT: A new nonlinear optical crystal, $\text{Na}_3\text{VO}_2\text{B}_6\text{O}_{11}$, has been grown by the top-seeded solution growth method using a $\text{Na}_2\text{CO}_3\text{--V}_2\text{O}_5$ flux. The structure of the compound was determined by single-crystal X-ray diffraction. It crystallizes in the noncentrosymmetric orthorhombic system, space group $P2_12_12_1$, with cell parameters $a = 7.7359(9) \text{ \AA}$, $b = 10.1884(12) \text{ \AA}$, $c = 12.5697(15) \text{ \AA}$, $V = 990.7(2) \text{ \AA}^3$, and $Z = 4$. $\text{Na}_3\text{VO}_2\text{B}_6\text{O}_{11}$ has a three-dimensional structure consisting of hexaborate groups connected by VO_4 tetrahedra with the sodium atoms distributed in channels through out the three-dimensional network. The refractive indices have been measured by the minimum deviation technique and fit to the Sellmeier equations. Nonlinear optical measurements on the compound demonstrate that the material has second harmonic generation properties, with an efficiency approximately the same as that of KH_2PO_4 .

Introduction

Currently, intense research is underway into the study and development of new nonlinear optical (NLO) materials that exhibit highly efficient second harmonic generation (SHG) responses, especially in the blue region.^{1–3} In order for materials to give efficient SHG responses, they must be noncentrosymmetric (NCS).⁴ A variety of strategies have been put forth for designing new NCS materials that will give an observable bulk nonlinear susceptibility or enhance the prospects of NCS crystal packing.^{5,6} Since the NLO properties of crystals are related directly to the crystal structure, the combination of two different of anionic units in the same compound can be used to give rise to inorganic NLO materials with interesting properties, such as KTiOPO_4 , $\text{AMoO}_3(\text{IO}_3)$ ($A = \text{K, Rb, Cs}$), $\text{A}[\text{VO}_2(\text{IO}_3)_2]$ ($A = \text{K, Rb}$), $\text{A}[(\text{VO})_2(\text{IO}_3)_3\text{O}_2]$ ($A = \text{NH}_4, \text{Rb, Cs}$), and SrBPO_5 .^{7–10} These findings have prompted considerable interest in the synthesis of related compounds.

Borates with their outstanding properties have evoked wide interest as NLO materials.¹¹ Additionally, several vanadates, where V^{5+} is a d^0 transition metal (and strong distorter) that can promote the formation of new NCS materials, have been shown to have interesting NLO properties.^{12–15} Considering the excellent properties of borates and vanadates, we expect that the combination of the borate and the vanadate groups in the same crystal will produce a new class of NLO materials. Until now, there have been a few materials that contain both the borate and the vanadate group. Although few materials currently contain both borate and vanadate groups, an extensive search in the borate–vanadate system led to the finding of a new NLO crystal, $\text{Na}_3\text{VO}_2\text{B}_6\text{O}_{11}$ (NVB).

NVB was first reported by Touboul et al.,¹⁶ and to our best knowledge, no additional studies on the NVB compound have been reported until now. The majority of NLO materials currently used as devices are fabricated from bulk single crystals.¹⁷ In this contribution, the synthesis, crystal growth, structure, and optical properties of the NVB crystal are reported.

Experimental Procedures

Synthesis and Crystal Growth. Polycrystalline samples of NVB were synthesized by traditional solid-state reaction. Stoichiometric amounts of Na_2CO_3 (Tianjin Benchmark Chemical Reagent Co., Ltd., 99.8%), V_2O_5 (Shanghai Shanpu Chemical Co., Ltd., 99.5%), and H_3BO_3 (Tianjin Baishi Chemical Industry Co., Ltd., 99.5%) were ground together and then packed into a Pt crucible. The temperature was raised to 500 °C at a rate of 2 °C/min in order to avoid ejection of starting materials from the crucible owing to vigorous evolution of CO_2 and H_2O . After preheating at 500 °C for 10 h, the sample was cooled to room temperature and ground up again. The sample was then calcined at 600 °C for two days with several intermediate grindings until a monophasic powder was achieved. The phase purity of NVB was confirmed by powder X-ray diffraction (XRD) (See Figures 1 and 2).

The NVB crystals were grown using a $\text{Na}_2\text{CO}_3\text{--V}_2\text{O}_5$ flux. A Pt crucible containing Na_2CO_3 , V_2O_5 , and H_3BO_3 in the molar ratio of 5:2:12 was placed in the center of a vertical, programmable temperature furnace. The mixture was heated to 850 °C and held at this temperature for 15 h to melt the powders into a liquid solution. A Pt wire was dipped into the 850 °C solution, and the temperature was decreased to room temperature at a rate of 1 °C/h. This resulted in high-quality NVB seed crystals grown by spontaneous nucleation along the Pt wire during the slow cooling process. The top seeded solution growth method was employed to grow large single crystals of NVB. A seed crystal of NVB was attached with Pt wire to an alumina rod and then suspended in a Na_2CO_3 , V_2O_5 , and H_3BO_3 solution at 850 °C containing the same molar ratios used to grow the seed crystals. Crystals were grown by cooling at a rate of 1 °C/day until the desired size was obtained.

*E-mail: slpan@ms.xjb.ac.cn. Phone: (86)991-3674558 Fax: (86)991-3838957.

X-ray Crystallography. Powder XRD was performed on Bruker D8 ADVANCE X-ray diffractometer equipped with a diffracted-beam monochromator set for Cu K α radiation ($\lambda = 1.5418 \text{ \AA}$). Single-crystal XRD data were collected on a Bruker SMART APEX II CCD X detector using graphite-monochromated Mo K α radiation ($\lambda = 0.71073 \text{ \AA}$) and integrated with the *S SAINT-Plus* program.¹⁸ A colorless and transparent crystal with dimensions $0.32 \times 0.23 \times 0.07 \text{ mm}^3$ was chosen for structure determination, and unit cell parameters were derived from a least-squares analysis of 9157 reflections in the range $2.57^\circ < \theta < 28.25^\circ$. All calculations were performed with programs from the *SHELXTL-97* crystallographic software package.¹⁹ The crystal structure of the compound was solved in space group $P2_12_12_1$. Final least-squares refinement on F_o^2 with data having $F_o^2 \geq 2\sigma(F_o^2)$ includes anisotropic displacement parameters for all atoms. The final difference Fourier synthesis map showed the maximum and minimum peaks at 0.317 and -0.433 e/\AA^3 , respectively. The structure was checked for missing symmetry elements with *PLATON*.²⁰ Crystal data and structure refinement information are summarized in Table 1. Final atomic coordinates and equivalent isotropic displacement parameters of the title compound are listed in Table S1 in the Supporting

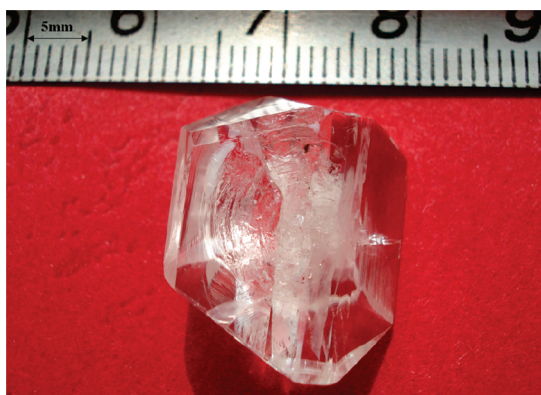


Figure 1. Photograph of the NVB crystal grown by the top-seeded solution growth method.

Information. Selected interatomic distances and angles are given in Table S2 in the Supporting Information.

Differential Thermal Analysis. The differential thermal analysis (DTA) curve for the NVB crystals was recorded with a simultaneous thermal analyzer, NETZSCH STA 449C. The sample was placed in an Al_2O_3 crucible and heated at a rate of $10^\circ\text{C min}^{-1}$ in the range of $25\text{--}900^\circ\text{C}$ under flowing nitrogen gas.

Elemental Analysis. The summary of ICP elemental analysis of Na, V, and B was performed using a Varian Vita-Pro CCD

Table 1. Crystal Data and Structure Refinement for the NVB Crystal

| | |
|--|--|
| empirical formula | $\text{Na}_3\text{VO}_2\text{B}_6\text{O}_{11}$ |
| formula weight | 392.77 |
| temp, K | 273(2) |
| crystal system | orthorhombic |
| space group | $P2_12_12_1$ |
| unit cell dimensions, \AA | $a = 7.7359(9)$ $b = 10.1884(12)$ $c = 12.5697(15)$ |
| vol, \AA^3 | 990.7(2) |
| Z | 4 |
| density (calcd), g/cm^3 | 2.633 |
| abs coeff, mm^{-1} | 1.215 |
| $F(000)$ | 760 |
| crystal size, mm^3 | $0.32 \times 0.23 \times 0.07$ |
| θ range (deg) for data collection | $2.57\text{--}28.25$ |
| index ranges | $-10 \leq h \leq 10, -13 \leq k \leq 13, -16 \leq l \leq 16$ |
| reflns collected | 9157 |
| completeness (%) to $\theta = 28.25^\circ$ | 99.9 |
| refinement method | full-matrix least-squares on F^2 |
| data/restraints/params | 2442/0/209 |
| GOF on F^2 | 1.075 |
| final R indices | $R_1 = 0.0252, wR_2 = 0.0673$ |
| $[F_o^2 > 2\sigma(F_o^2)]^a$ | |
| R indices (all data) ^a | $R_1 = 0.0274, wR_2 = 0.0693$ |
| extinction coeff | 0.0078(11) |

$$^a R_1 = \frac{\sum ||F_o| - |F_c||}{\sum |F_o|} \text{ and } wR_2 = \left[\frac{\sum w(F_o^2 - F_c^2)^2}{\sum wF_o^4} \right]^{1/2} \text{ for } F_o^2 > 2\sigma(F_o^2).$$

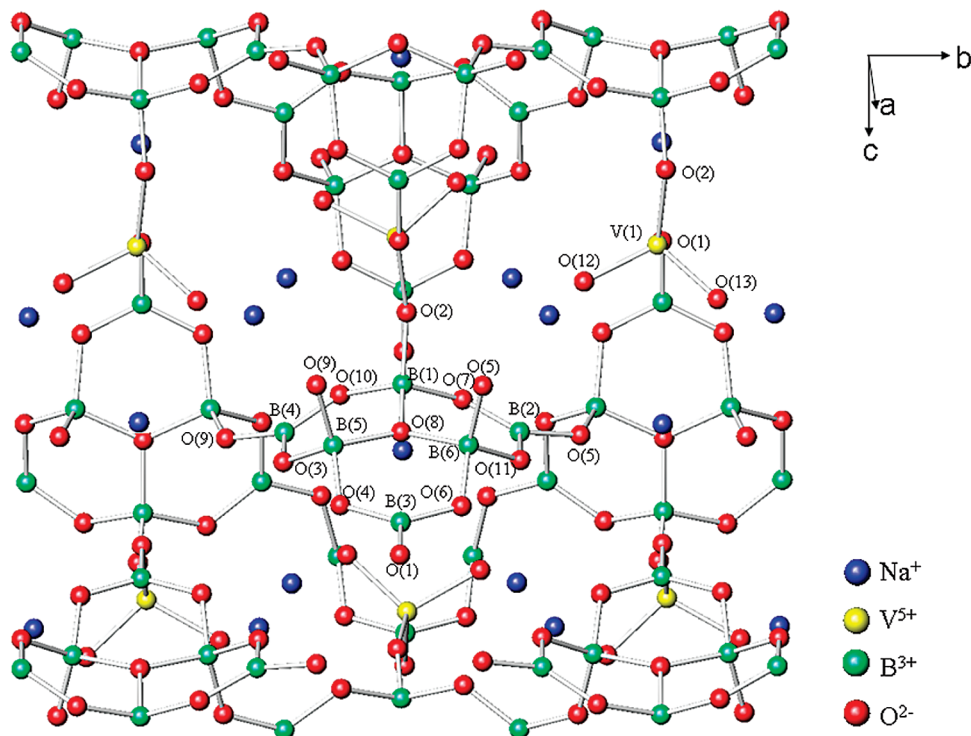


Figure 2. Ball-and-stick representation of the NVB compound. The sodium atoms distributed in the channels of the three-dimensional network. One of the VO_4 units and one of the hexaborate groups are labeled.

Table 2. Refractive Indices for the NVB Crystal

| λ (μm) | n_x | | | n_y | | | n_z | | |
|-----------------------------|---------|---------|----------|---------|---------|----------|---------|---------|----------|
| | exptl | calcd | errors | exptl. | calcd. | errors | exptl. | calcd. | errors |
| 0.4358 | 1.63649 | 1.65154 | -0.01506 | 1.68498 | 1.67818 | 0.00681 | 1.68036 | 1.68036 | 0.00000 |
| 0.4861 | 1.62371 | 1.62362 | 0.00009 | 1.66927 | 1.66727 | 0.00200 | 1.66789 | 1.66791 | -0.00002 |
| 0.5461 | 1.61883 | 1.61836 | 0.00047 | 1.66232 | 1.66258 | -0.00026 | 1.66690 | 1.66688 | 0.00002 |
| 0.5790 | 1.61576 | 1.61550 | 0.00026 | 1.65917 | 1.65962 | -0.00045 | 1.65868 | 1.65874 | -0.00007 |
| 0.5893 | 1.61493 | 1.61458 | 0.00034 | 1.65826 | 1.65865 | -0.00039 | 1.65527 | 1.65516 | 0.00012 |
| 0.6563 | 1.60728 | 1.60830 | -0.00102 | 1.65263 | 1.65187 | 0.00076 | 1.65415 | 1.65418 | -0.00002 |
| 0.6943 | 1.60493 | 1.60446 | 0.00046 | 1.64737 | 1.64767 | -0.00030 | 1.64892 | 1.64898 | -0.00005 |

simultaneous ICP-OES spectrometer. Found: Na, 17.78; V, 13.01; B, 17.05%. Calcd for NVB: Na, 17.56; V, 12.97; B, 16.51%.

Second-Order NLO Measurements. Powder second harmonic generation (SHG) measurements were carried out on the NVB sample using the Kurtz and Perry method.²¹ About 80 mg of powder was pressed into a pellet, which was then irradiated with a pulsed infrared beam (10 ns, 10 kHz) produced by a Q-switched Nd:YAG laser of wavelength 1064 nm. A 532 nm filter was used to absorb the fundamental and pass the visible light onto a photomultiplier. A combination of a half-wave achromatic retarder and a polarizer was used to control the intensity of the incident power, which was measured with an identical photomultiplier connected to the same high-voltage source. This procedure was then repeated using a standard NLO material, in this case microcrystalline KH_2PO_4 (KDP), and the ratio of the second harmonic intensity outputs was calculated. Because the SHG efficiency has been shown to depend strongly on particle size,²² polycrystalline NVB was ground and sieved into distinct particle size ranges, < 20, 20–38, 38–55, 55–88, 88–105, 105–150, and 150–200 μm . To make relevant comparisons with known SHG materials, we also ground and sieved crystalline SiO_2 and KDP into the same particle size ranges.

Transmission Spectrum Measurement. The transmission spectrum of the NVB crystal was recorded at room temperature using a Lambda 900UV/VIS/NIR (Perkin-Elmer) spectrophotometer. The measurement range extended from 185 to 3000 nm.

Refractive Indices Measurement. The refractive indices dispersion of NVB was determined by the minimum deviation technique at seven different wavelengths between 435.8 and 694.3 nm. Since NVB is a biaxial crystal with point group symmetry $P2_12_12_1$, it is possible to measure n_x , n_y , and n_z using two prisms. The values of room temperature refractive indices for n_x , n_y , and n_z measured at specific wavelengths are summarized in Table 2.

Results and Discussion

The DTA curve of NVB is shown in Figure S3 in the Supporting Information. There are two endothermic peaks on the heating curve, suggesting that NVB melts incongruently and, therefore, requires the use of a flux for single crystal growth. A colorless and transparent NVB crystal with dimensions $18 \times 12 \times 5 \text{ mm}^3$ (Figure 1) has been grown by the top-seeded solution growth method. It shows that the crystal exhibits fairly distinguishable facets. The NVB crystal has a moderate hardness of approximately 5.5 on the Mohs scale, so during the growth, cutting, and polishing processes, it did not crack. The NVB crystal was also very stable in air and in moist environments, which demonstrated that it is chemically stable and not hygroscopic.

NVB consists of a three-dimensional structure composed of hexaborate groups connected by VO_4 tetrahedra with the sodium atoms distributed in the channels of the three-dimensional network (see Figure 2). The coordination of sodium atoms with oxygen atoms is shown in Figure S4 in the Supporting Information. The three BO_4 units are joined together through corner-sharing the O(8) atom; the three BO_4 units and three BO_3 units formed a compact hexaborate unit. Except for the O(12) and O(13) atoms (see Figure 2), all the others are borate oxygens. As a result, the

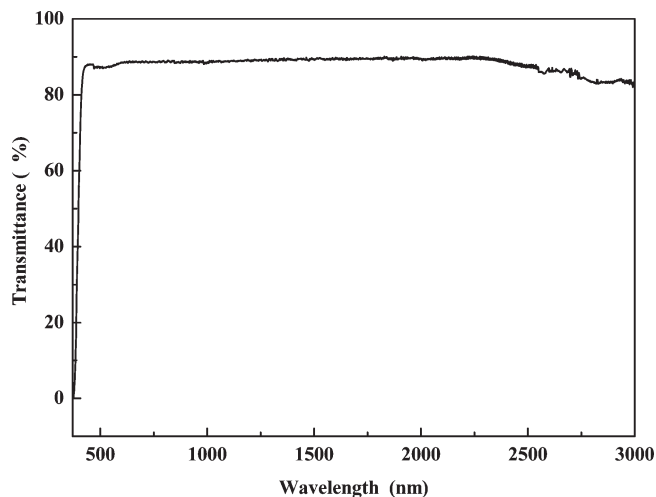


Figure 3. Transmittance spectrum of the NVB crystal.

NVB compound is an oxy-borate, which can be formulated as $\text{Na}_3\text{VO}_2\text{B}_6\text{O}_{11}$.

The bond valence sums of each atom in NVB are calculated^{23,24} and listed in Table S3 in the Supporting Information. These charges, based on the bond lengths determined by the X-ray structure analysis, are in agreement with the expected oxidation states.

Optical properties were measured on a single crystal. Samples 0.8 mm in thickness were cut from the as-grown crystal and then polished on diamond-impregnated laps. The transmittance spectrum was recorded with the (001) face at the incident surface. As shown in Figure 3, it can be seen that a wide transmission range is observed from 370 to 3000 nm with the UV absorption edge at about 370 nm; the transmission is above 80% between 412 and 3000 nm. There are no absorption peaks in the whole range of the spectrum, but the transmission intensity sharply decreases below 412 nm and reaches zero at about 370 nm. This means that the ultraviolet cutoff edge for the NVB crystal is 370 nm.

Determination of Sellmeier equations is needed for further prediction of the shortest SHG wavelength and the phase-matching directions.²⁵ The Sellmeier equations, which are fit with the above measured refractive indices, are as follows:

$$n_x^2 = 2.57017 + 0.01590907/(\lambda^2 - 0.05571750) - 0.04018709\lambda^2$$

$$n_y^2 = 2.58674 + 0.01977298/(\lambda^2 - 0.04197894) - 0.01889726\lambda^2$$

$$n_z^2 = 2.67886 + 0.01864372/(\lambda^2 - 0.06518985) - 0.02493503\lambda^2$$

where λ is the wavelength expressed in micrometers. The calculated and experimental values are consistent and match to the third decimal place. NVB is a positive biaxial optical crystal, and the birefringence value is around 0.042 over the

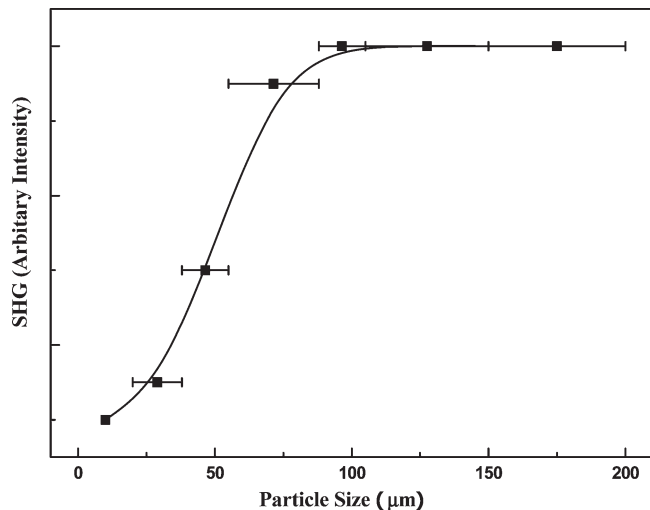


Figure 4. Phase-matching curve, that is, particle size vs SHG intensity, for NVB crystal is given. The curve drawn is to guide the eye and is not a fit to the data.

measured wavelength region. On the basis of the Sellmeier equations, the phase-matching curves for SHG can be calculated with the shortest SHG wavelength for NVB at 427 nm for type I phase matching. Therefore, the SHG of a Nd:YAG laser radiation (1064 nm) is possible for type I phase matching, and the phase-matching angles for type I SHG of 1064 nm calculated from the Sellmeier equations are $\theta = 79.3^\circ$, $\varphi = 0^\circ$, and $\theta = 47.5^\circ$, $\varphi = 90^\circ$.

Since NVB crystallizes in the NCS space group, $P2_12_12_1$, SHG measurements were carried out (see Figure 4). The crystal grown by the top-seeded solution growth method was ground into powder and loaded into a quartz cell. Our preliminary studies show that green light was observed and its intensity was similar to that of KDP. Therefore, this demonstrates that the powder SHG effect of NVB is about the same as that of KDP. Additionally, phase-matching experiments, that is, particle size vs SHG efficiency, indicate that the material is phase-matchable. According to the literature,²⁶ the relationship of the second-order NLO susceptibility in the borate anions is $\chi(\text{BO}_3)^{3-} \gg \chi(\text{BO}_4)^{5-}$. The d^0 transition metal V^{5+} (strong distorter) in the VO_4 asymmetric coordination environments can also bring out a large second-order NLO susceptibility.^{14,15} Thus, the SHG response of NVB is considered to be primarily attributed to the VO_4 tetrahedra and the BO_3 triangles, while a smaller contribution to the SHG response is assumed to be associated with the BO_4 tetrahedra in the structure. Therefore, the combination of borate and vanadate units would make a significant contribution to the second-order NLO susceptibility of NVB.

Conclusions

A new NLO crystal, $\text{Na}_3\text{VO}_2\text{B}_6\text{O}_{11}$, crystallizes in the space group $P2_12_12_1$ with cell dimensions $a = 7.7359(9)$ Å, $b = 10.1884(12)$ Å, and $c = 12.5697(15)$ Å. Crystals with approximate dimensions $18 \times 12 \times 5$ mm³ have been grown by the top-seeded solution growth method using a Na_2CO_3 – V_2O_5 flux. The NLO properties measured indicate that the compound is phase-matchable and gives a similar response to that of KDP. NVB has a wide transparency range from 370 to 3000 nm with the shortest SHG wavelength at 427 nm, which demonstrates that it has potential as a SHG material for blue

wavelength applications. A moderate birefringence with good chemical stability and mechanical durability makes NVB a promising NLO material. Our results are believed to be valuable in the search and design of new inorganic NLO materials.

Acknowledgment. This work is supported by the National Natural Science Foundation of China (Grant No. 50802110), the Natural Science Foundation of Xinjiang Uygur Autonomous Region of China (Grant No. 200821159), Youth Science Foundation of Xinjiang Uygur Autonomous Region of China (Grant No. 2009211B33), the One Hundred Talents Project Foundation Program, the Western Light Joint Scholar Foundation Program of Chinese Academy of Sciences, and the High Technology Research and Development Program of Xinjiang Uygur Autonomous Region of China (Grant No. 200816120).

Supporting Information Available: Calculated and observed X-ray diffraction pattern data, an X-ray crystallographic file in CIF format including complete crystallographic details, interatomic distances and angles for NVB, XRD pattern data, the coordination of sodium atoms with oxygen atoms, DTA curve of NVB, phase-matching curve of KDP sample, non-phase-matching curve of SiO_2 sample, and bond valence analysis of the NVB. This material is available free of charge via the Internet at <http://pubs.acs.org>.

References

- (1) (a) Becker, P. *Adv. Mater.* **1998**, *10*, 979. (b) Chen, C. T.; Wang, Y. B.; Wu, B. C.; Wu, K. C.; Zeng, W. L.; Yu, L. H. *Nature* **1995**, *373*, 322. (c) Knyrim, J. S.; Becker, P.; Johrendt, D.; Huppertz, H. *Angew. Chem., Int. Ed.* **2006**, *45*, 8239.
- (2) (a) Keszi, D. A. *Curr. Opin. Solid State Mater. Sci.* **1999**, *4*, 155. (b) Sasaki, T.; Mori, Y.; Yoshimura, M.; Yap, Y. K.; Kamimura, T. *Mater. Sci. Eng. R* **2000**, *30*, 1.
- (3) (a) Cheng, L. T.; Cheng, L. K.; Harlow, R. L.; Bierlein, J. D. *Appl. Phys. Lett.* **1994**, *64*, 155. (b) Pan, S. L.; Smit, J. P.; Watkins, B.; Marvel, M. R.; Stern, C. L.; Poepelmeier, K. R. *J. Am. Chem. Soc.* **2006**, *128*, 11631.
- (4) (a) Sivakumar, T.; Chang, H. Y.; Baek, J.; Halasyamani, P. S. *Chem. Mater.* **2007**, *19*, 4711. (b) Ra, H. S.; Ok, K. M.; Halasyamani, P. S. *J. Am. Chem. Soc.* **2003**, *125*, 7764. (c) Mezei, G.; Kampf, J. W.; Pan, S. L.; Poepelmeier, K. R.; Watkins, B.; Pecoraro, V. L. *Chem. Commun.* **2007**, *11*, 1148.
- (5) Halasyamani, P. S.; Poepelmeier, K. R. *Chem. Mater.* **1998**, *10*, 2753.
- (6) (a) Zyss, J.; Oudar, J. L. *Phys. Rev. A* **1982**, *26*, 2028. (b) Guloy, A. M.; Tang, Z. J.; Miranda, P. B.; Srdanov, V. I. *Adv. Mater.* **2001**, *13*, 833.
- (7) Phillips, M. L.; Harrison, W. T.; Stucky, G. D.; McCarron, E. M., III; Calabrese, J. C.; Gier, T. E. *Chem. Mater.* **1992**, *4*, 222.
- (8) Sykora, R. E.; Ok, K. M.; Halasyamani, P. S.; Albrecht-Schmitt, T. E. *J. Am. Chem. Soc.* **2002**, *124*, 1951.
- (9) Sykora, R. E.; Ok, K. M.; Halasyamani, P. S.; Wells, D. M.; Albrecht-Schmitt, T. E. *Chem. Mater.* **2002**, *14*, 2741.
- (10) Pan, S. L.; Wu, Y. C.; Fu, P. Z.; Zhang, G. C.; Li, Z. H.; Du, C. X.; Chen, C. T. *Chem. Mater.* **2003**, *15*, 2218.
- (11) (a) Chen, C. T.; Wu, B. C.; Jiang, A. D.; You, G. M. *Sci. Sin.* **1985**, *B18*, 235. (b) Chen, C. T.; Wu, B. C.; Jiang, A. D.; You, G. M.; Li, R.; Lin, S. J. *J. Opt. Soc. Am.* **1989**, *B6*, 616. (c) Wu, Y. C.; Sasaki, T.; Nakai, S.; Yokotani, A.; Tang, H.; Chen, C. T. *Appl. Phys. Lett.* **1993**, *62*, 2614. (d) Yoshimura, M.; Mori, Y.; Sasaki, T. *Opt. Mater.* **2004**, *26*, 421. (e) Li, F.; Hou, X. L.; Pan, S. L.; Wang, X. A. *Chem. Mater.* **2009**, *21*, 2846. (f) Lin, Z. S.; Lin, J.; Wang, Z. Z.; Chen, C. T. *Phys. Rev. B* **2000**, *62*, 1757.
- (12) (a) Terada, Y.; Shimamura, K.; Kochrikhin, V. V.; Barashov, L. V.; Ivanov, M. A.; Fukuda, T. *J. Cryst. Growth* **1996**, *167*, 369. (b) Maunier, C.; Doualan, J. L.; Moncorge, R.; Speghini, A.; Bettinelli, M.; Cavalli, E. *J. Opt. Soc. Am.* **2002**, *B19*, 1794. (c) Pless, J. D.; Erdman, N.; Ko, D.; Marks, L. D.; Stair, P. C.; Poepelmeier, K. R. *Cryst. Growth Des.* **2003**, *3*, 615. (d) Jiang, H. L.; Ma, E.; Mao, J. G. *Inorg. Chem.* **2007**, *46*, 7012.

- (13) (a) Baudrin, E.; Denis, S.; Orsini, F.; Seguin, L.; Touboul, M.; Tarascon, J.-M. *J. Mater. Chem.* **1999**, *9*, 101. (b) Jiang, H. L.; Kong, F.; Fan, Y.; Mao, J. G. *Inorg. Chem.* **2008**, *47*, 7430.
- (14) (a) Halasyamani, P. S. *Chem. Mater.* **2004**, *16*, 3586. (b) Ok, K. M.; Halasyamani, P. S.; Casanova, D.; Llunell, M.; Alemany, P.; Alvarez, S. *Chem. Mater.* **2006**, *18*, 3176.
- (15) Sivakumar, T.; Chang, H. Y.; Baek, J.; Halasyamani, P. S. *Chem. Mater.* **2007**, *19*, 4711.
- (16) Touboul, M.; Penin, N.; Nowogrocki, G. *J. Solid State Chem.* **2000**, *150*, 342.
- (17) Hagerman, M. E.; Poepelmeier, K. R. *Chem. Mater.* **1995**, *7*, 602.
- (18) *SAlNT-Plus*, version 6.02A; Bruker Analytical X-ray Instruments, Inc.: Madison, WI, 2000.
- (19) Sheldrick, G. M. *SHELXTL*, version 6.14; Bruker Analytical X-ray Instruments, Inc.: Madison, WI, 2003.
- (20) Spek, A. L. *J. Appl. Crystallogr.* **2003**, *36*, 7.
- (21) Kurtz, S. Q.; Perry, T. T. *J. Appl. Phys.* **1968**, *39*, 3798.
- (22) Dougherty, J. P.; Kurtz, S. K. *J. Appl. Crystallogr.* **1976**, *9*, 145.
- (23) Brown, I. D.; Altermatt, D. *Acta Crystallogr.* **1985**, *B41*, 244.
- (24) Brese, N. E.; O'Keeffe, M. *Acta Crystallogr.* **1991**, *B47*, 192.
- (25) Fan, T. Y.; Huang, C. E.; Hu, B. Q.; Eckardt, R. C.; Fan, Y. X.; Byer, R. L.; Feigelson, R. S. *Appl. Opt.* **1987**, *26*, 2390.
- (26) (a) Chen, C. T.; Liu, G. Z. *Annu. Rev. Mater. Sci.* **1986**, *16*, 203. (b) Chen, C. T.; Ye, N.; Lin, J.; Jiang, J.; Zeng, W. Z.; Wu, B. C. *Adv. Mater.* **1999**, *11*, 1071.